

Wobbling phonon excitations in strongly deformed triaxial nuclei

G.B. Hagemann^a

The Niels Bohr Institute, University of Copenhagen, Blegdamsvej 17, DK-2100 Copenhagen Ø, Denmark

Received: 30 October 2002 /

Published online: 23 March 2004 – © Società Italiana di Fisica / Springer-Verlag 2004

Abstract. The wobbling mode is uniquely related to triaxiality and introduces a series of bands with increasing wobbling phonon number, n_w . The pattern of γ -transitions between the wobbling excitations will be influenced by the presence of an aligned particle. Evidence for the wobbling mode was obtained recently, and even a two-phonon wobbling excitation has now been identified in ^{163}Lu . The similarity of the data in ^{163}Lu to new strongly deformed triaxial bands and connecting transitions in the neighbouring nuclei, ^{165}Lu and ^{167}Lu , establishes wobbling as a more general phenomenon in this region. The higher phonon wobbling excitations show some anharmonicity, but the characteristic large $\Delta n_w = 1$ $E2$ strength is observed. The wobbling interpretation is based on the comparison of electromagnetic decay strength between bands to particle-rotor calculations in which an $i_{13/2}$ proton is coupled to a triaxial core.

PACS. 27.70.+q $150 \leq A \leq 189$ – 23.20.-g Electromagnetic transitions – 21.10.Re Collective levels

1 Introduction

Nuclei with $N \sim 94$ and $Z \sim 71$ provide a unique possibility of studying strongly deformed (SD) shapes with a pronounced triaxiality [1,2]. Calculations with the Ultimate Cranker (UC) code [3,4] based on a modified harmonic oscillator have revealed that large deformation minima are actually expected for all combinations of parity, π , and signature, α , in a region around the nuclei $^{163,165}\text{Lu}$ [5,6] where Triaxial Strongly Deformed (TSD) bands were first found [5,7,8]. As an example a potential energy surface for ^{163}Lu is shown in fig. 1. The $i_{13/2}$ proton orbital is involved in the intrinsic structure of the TSD bands observed in both even- and odd- N Lu isotopes.

Among the calculated, most favourable even-even Yb, Hf and W isotopes for finding low-lying TSD structures in the region are [6] $^{164,166}\text{Hf}$. It appears that in spite of various searches in Hf nuclei no examples of TSD band structures could be found in those isotopes, whereas there is experimental evidence for three weakly populated TSD bands in ^{168}Hf , for which lifetime measurements have confirmed the large deformation [9]. The search for TSD bands in the region has been extended to heavier Hf's as well as to neighbouring Lu isotopes. Also new lifetime measurements have been initiated to substantiate the expected large deformations.

A proof of nuclear triaxiality in the region was recently obtained by the evidence for the wobbling mode in ^{163}Lu [10–12]. This mode is uniquely related to the triaxial nuclear shape and adds a new dimension to the

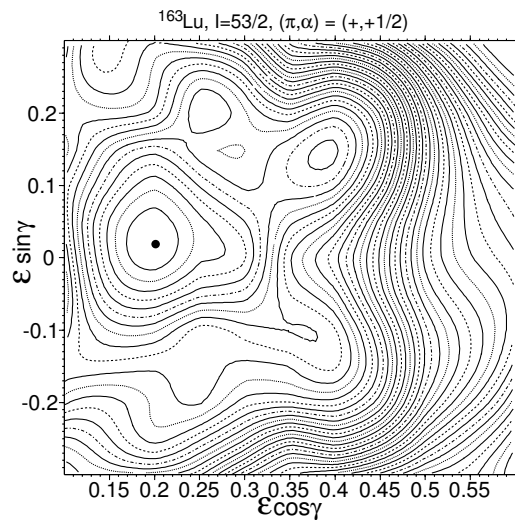


Fig. 1. Potential energy surface for ^{163}Lu for parity and signature $(\pi, \alpha) = (+, +1/2)$ at $I = 53/2\hbar$.

description of a rotating triaxial nucleus. The rotational motion of a triaxial deformed nucleus with moments of inertia, $\mathcal{J}_x > \mathcal{J}_y, \mathcal{J}_z$ induces in the high spin limit, $I \gg 1$, a sequence of wobbling bands described by the energy, $E_R(I, n_w) = I(I+1)/2\mathcal{J}_x + \hbar\omega_w(n_w + 1/2)$, where n_w is the wobbling phonon number and the wobbling frequency, $\hbar\omega_w = \hbar\omega_{\text{rot}} \sqrt{(\mathcal{J}_x - \mathcal{J}_y)(\mathcal{J}_x - \mathcal{J}_z)/(\mathcal{J}_y\mathcal{J}_z)}$ with $\hbar\omega_{\text{rot}} = I\hbar^2/\mathcal{J}_x$ [13]. A family of wobbling bands is expected to have a very similar intrinsic structure. The

^a e-mail: hagemann@nbi.dk

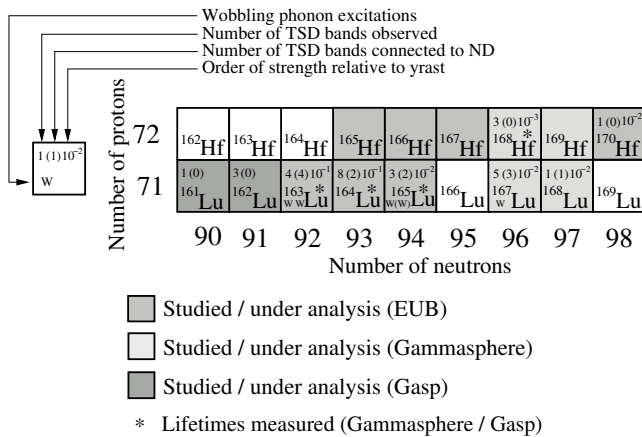


Fig. 2. Overview of searches and results for Lu and Hf nuclei. References for the individual nuclei are: ^{161,162}Lu [14], ¹⁶³Lu [7, 10–12, 15], ¹⁶⁴Lu [16], ¹⁶⁵Lu [5, 17], ¹⁶⁷Lu [18, 19], ¹⁶⁸Lu [20], ¹⁶⁶Hf [21], ¹⁶⁸Hf [9] and ¹⁷⁰Hf [22]. References for lifetime measurements on TSD bands are: ^{163,164,165}Lu [8, 23, 24] and ¹⁶⁸Hf [9].

presence of an aligned particle influences both $E2$ and $M1$ matrix elements for transitions between the bands, and the evidence for wobbling is based on the comparison of the strength of γ -transitions between the wobbling excitations to particle-rotor calculations in which an $i_{13/2}$ proton is coupled to a triaxial core [25].

The implications introduced by the wobbling mode including the recent evidence for the one- and two-phonon wobbling excitations in ¹⁶³Lu are presented, after giving an overview of experimental results on TSD bands in the Lu-Hf region.

2 Structures of TSD bands in Hf-Lu nuclei

The Lu-Hf nuclei have been the subject for extensive spectroscopic investigations with the aim of understanding the underlying structure in the strongly deformed triaxial well, exemplified in fig. 1, since the first established $\pi i_{13/2}$ TSD band was found in ¹⁶³Lu [7, 8]. Figure 2 gives a schematic overview of these investigations and the results obtained. In addition, very recently a EUROBALL experiment with the aim of studying further the bands found in ^{161,162}Lu has been performed, and a recent finding of four weakly populated, yet unconnected bands in ¹⁷⁴Hf extends the region to a considerably higher neutron number [26]. For many of the recent results presented at this conference, refer to refs. [12, 14, 17, 22]. Although the region now counts more than 20 bands, presumably of TSD structure, only a few of them have been connected to known normal deformed states, and have therefore known excitation energy and, possibly, spin and parity firmly assigned.

In the even- N Lu isotopes the yrast TSD band, with positive parity and signature, $\alpha = +1/2$ are interpreted as based on an $i_{13/2}$ proton. This particle is also involved in the two connected TSD bands in odd-odd ¹⁶⁴Lu. For most of the bands referred to in fig. 2 the TSD structure

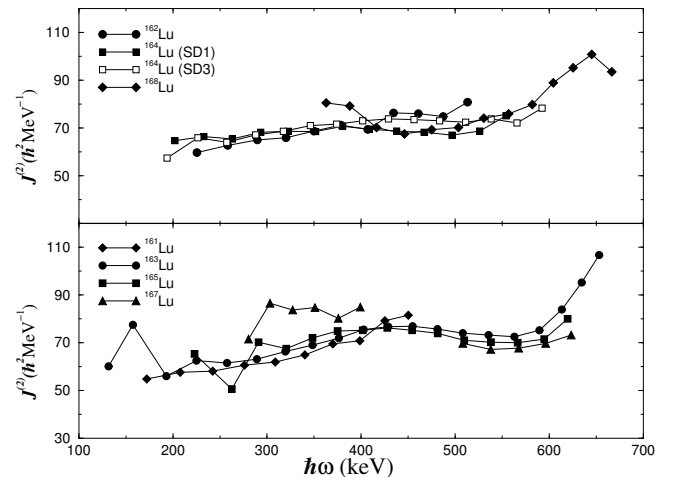


Fig. 3. Dynamic moments of inertia for odd- and even- N Lu isotopes. References for the individual nuclei are given in the caption to fig. 2 For ¹⁶⁷Lu the region of a crossing is omitted, see text below.

is inferred from the similarity of the dynamic moment of inertia, $\mathcal{J}^{(2)}$, to values obtained for ¹⁶³Lu. They appear fairly constant with frequency over a large range in spin, and larger than values for the ND bands when compared in regions of frequency avoiding crossings in the ND bands. As an example values of $\mathcal{J}^{(2)}$ for the yrast TSD band in the even- N Lu isotopes together with the lowest TSD bands in odd-odd Lu isotopes are shown in fig. 3. For the even- N Lu-isotopes in the lower panel of fig. 3 there is a clear systematic trend with neutron number, in the frequency dependence of $\mathcal{J}^{(2)}$, which might be caused by the approach of the neutron Fermi level to the strongly deformation driving $j_{15/2}$ sub-shell. A rise at high frequency seems general, and therefore most likely related to an alignment in the proton system. For TSD1 in ¹⁶⁸Hf and the newly found TSD band in ¹⁷⁰Hf [22] the $\mathcal{J}^{(2)}$ values resemble those of ^{163,165}Lu.

The mechanisms behind the decay-out from a potential well of a different shape, as the case for the local minimum at $(\varepsilon_2, \gamma) \sim (0.4, 19^\circ)$ in fig. 1, to the normal-deformed well will depend on the excitation energy of the well and the height of the barrier between the two minima. Decay-out of superdeformed bands is a subject of considerable interest. The few cases found are interpreted as mainly of “statistical” character.

In the cases where the decay-out of TSD bands have been established two different scenarios are present. The decay-out observed in ¹⁶⁴Lu from TSD1 and TSD3 [16] comprises both stretched and unstretched $E1$ and $E2$ transitions in the energy range ~ 0.9 – 1.5 MeV, most likely of “statistical” nature. In contrast, the decay-out from TSD1 in ¹⁶³Lu at $I = 25/2$ and $21/2$ (see fig. 4) can be completely explained by mixing at $I = 21/2$, where the level distance is ~ 110 keV, with a rather large interaction (~ 22 keV). Since the band TSD1 comes considerably closer to ND structures at higher spin with no observation of cross-band transitions, one may conclude that the barrier is probably more efficient in separating the

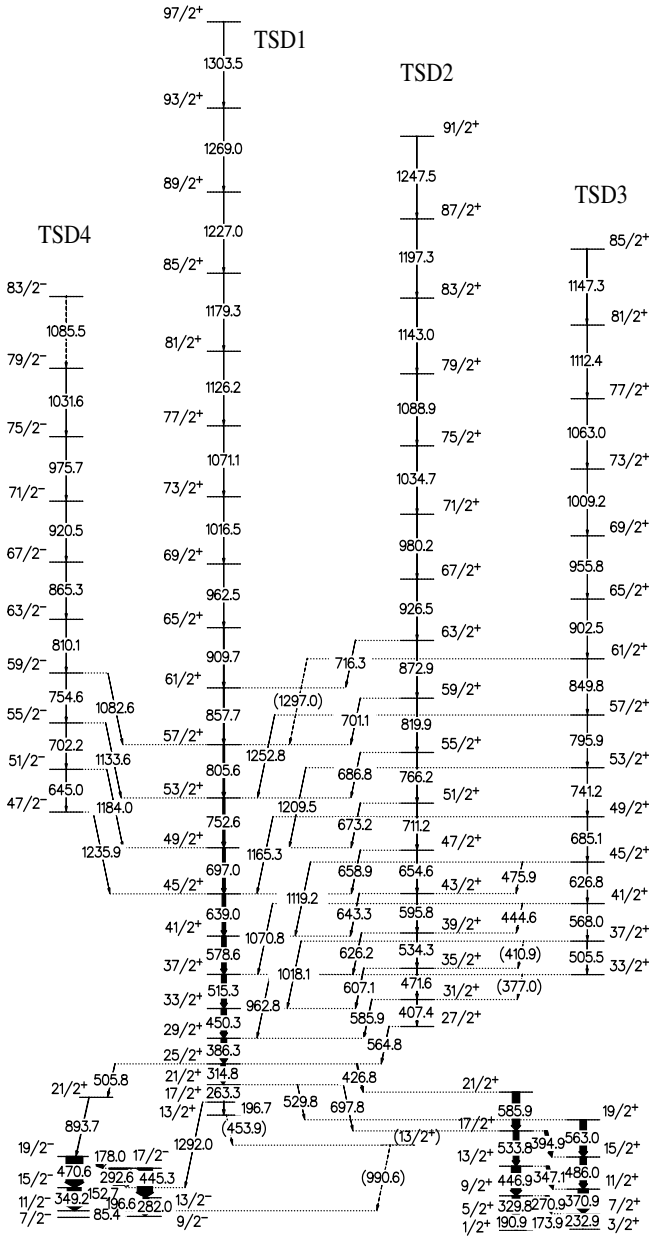


Fig. 4. Partial level scheme of ^{163}Lu showing three TSD bands together with the connecting transitions to the ND structures to which the TSD states decay [11, 12, 15, 27].

two minima at higher spin values, which also agrees with calculations. The different branching ratios also contain information on the ratio, $Q_t(\text{TSD})/Q_t(\text{ND}) \sim 2$, which confirms the larger deformation of TSD1 [15]. The weak $E1$ decay observed from $I = 17/2\hbar$ resembles the $E1$ decays observed in ^{164}Lu .

In addition, data from GAMMASPHERE on the decay-out in $^{167,168}\text{Lu}$ [19, 20], and, new data from a recent EUROBALL experiment in ^{165}Lu [17] show that in both of these even- N Lu isotopes the decay-out of the yrast TSD band occurs through mixing, like in ^{163}Lu . In ^{167}Lu the TSD and ND bands cross and interact at intermediate

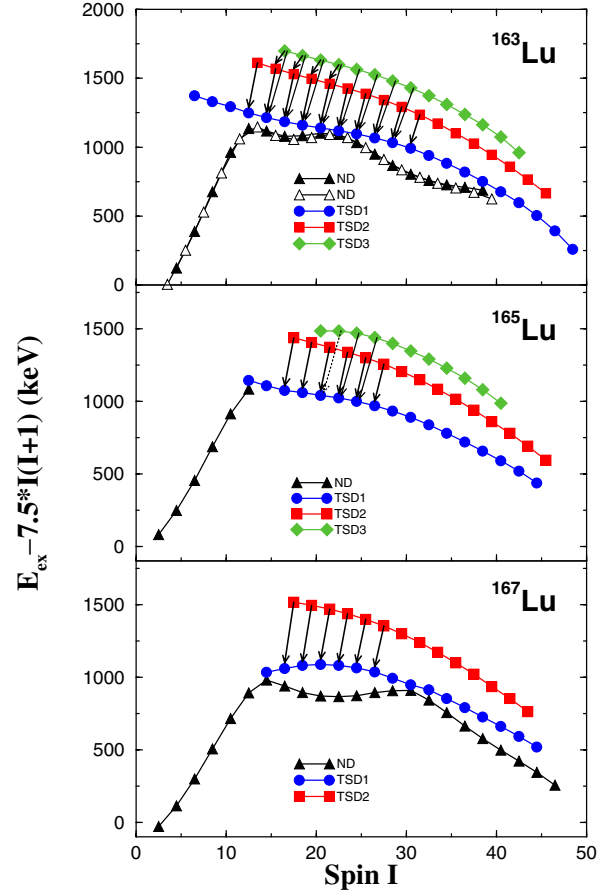


Fig. 5. Excitation energy relative to a rigid reference of the TSD bands together with normal-deformed bands in ^{163}Lu (top), ^{165}Lu (middle) and ^{167}Lu (bottom). The decays from the excited TSD bands to the yrast TSD1 are indicated with arrows.

as well as at low spin, see fig. 5, bottom part. The irregularities at low frequency for $^{163,165,167}\text{Lu}$ are in fact caused by these interactions with ND states at lower spin. The frequency range disturbed by the interaction at intermediate spin for ^{167}Lu is removed from the figure. For ^{161}Lu no decay-out has been firmly established so far, but it seems from the regular behavior of the dynamic moment of inertia that decay-out in this nucleus is not caused by mixing, in contrast to the case for $^{163,165,167}\text{Lu}$. With these different examples we conclude that the preferred decay-out of a particular TSD band will depend on the excitation energy relative to the available ND bands with which the TSD states may mix at their closest mutual distance.

The best studied nucleus in the region is ^{163}Lu , which has four connected TSD bands, [10–12, 15, 27]. The most striking feature of the level scheme of ^{163}Lu , shown in fig. 4, is maybe that the decay of the excited TSD bands all proceed through the yrast TSD band, TSD1. In addition, the three bands, TSD1, TSD2 and TSD3 have very similar dynamic moments of inertia and alignments over almost the full frequency range. The multipolarity of the transitions from TSD2, TSD3 and TSD4 to TSD1 and from TSD3 to TSD2 have been determined by the analysis

Table 1. Experimental values of angular-distribution ratios $\frac{W(25)}{W(90)}$, DCO ratios (gated on stretched $E2$ transitions), mixing ratios $\langle\delta\rangle$ and $\frac{B(E2)_{\text{out}}}{B(E2)_{\text{in}}}$ for $\Delta I = 1$ transitions between TSD bands in ^{163}Lu [12]. Values for TSD2 \rightarrow TSD1 are averaged over transitions with $17.5 \leq I_i \leq 27.5$ while the values for TSD3 \rightarrow TSD2 correspond to $I_i = 22.5$.

Trans.	$\frac{W(25)}{W(90)}$	DCO ratio	$\langle\delta\rangle$	$\frac{B(E2)_{\text{out}}}{B(E2)_{\text{in}}}$
2 \rightarrow 1	0.46(5)	0.33(3)	$-3.1^{+0.36}_{-0.44}$	0.21 ± 0.01
3 \rightarrow 2	0.49(10)	0.38(11)	$-3.6^{+0.97}_{-1.93}$	0.51 ± 0.13
–	–	–	$-0.19^{+0.08}_{-0.12}$	$0.019^{+0.024}_{-0.017}$

of Directional Correlation from Oriented states and angular distribution ratios, as well as linear polarization, for the strongest of the transitions. It has thereby been possible to assign firm spin and positive parity to TSD2 and TSD3, whereas TSD4, decaying to TSD1 with stretched dipole transitions presumably has negative parity [27]. With very similar experimental features of the positive parity bands, TSD1, TSD2 and TSD3 a pattern compatible with expectations from wobbling phonon excitations has emerged [10–12, 25]. In contrast, TSD4 with negative parity has $\sim 2\hbar$ larger alignment than TSD1–3, most likely corresponding to the lowest expected three-quasiparticle configuration with $(\pi, \alpha) = (-, -1/2)$ in the triaxial well.

The mixing ratios averaged over the $\Delta I = 1$ transitions TSD2 \rightarrow TSD1 give, together with the measured branching ratios, rather large values of $B(E2)_{\text{out}}/B(E2)_{\text{in}}$ (see table 1). For the $\Delta I = 1$ transitions to TSD2 from TSD3, which has a weaker population, only one value could be extracted, and a polarization analysis has not been possible. Based on the close similarity to the quantities for the TSD2 \rightarrow TSD1 transitions, given in table 1, we assume that the larger negative value for the mixing ratio δ is the valid solution, resulting in an even larger value of $B(E2)_{\text{out}}/B(E2)_{\text{in}}$. With such large $E2$ transition matrix elements between these bands an interpretation in terms of quasiparticle excitations in the triaxial well becomes very difficult. In that scenario TSD2 would be the signature partner of TSD1, and TSD3 the lowest three-quasiparticle structure built on the $i_{13/2}$ proton coupled to 2 quasineutrons with signature $\alpha = 0$, for which the large values of $B(E2)_{\text{out}}/B(E2)_{\text{in}}$, as measured between them, would be most unlikely.

As illustrated in fig. 5, counterparts to TSD2 exist in both ^{165}Lu [17] and ^{167}Lu [19]. The $\Delta I = 1$ decays to the yrast TSD1, also have relative strengths and mixing ratios resembling those measured for ^{163}Lu . In addition, for ^{165}Lu a band similar to TSD3 in ^{163}Lu was found. Here the population was too weak, though, to establish the decay to TSD2, whereas $\Delta I = 2$ decays to TSD1 were found at very similar energies to those in ^{163}Lu .

3 The wobbling mode

The wobbling degree of freedom in an odd, triaxial nucleus like ^{163}Lu with aligned particle angular momentum

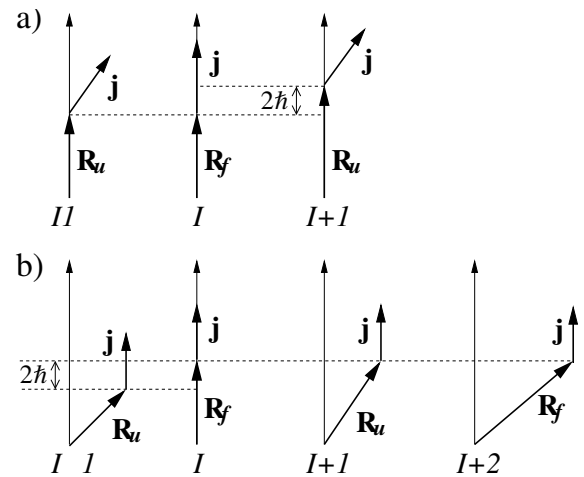


Fig. 6. Schematic coupling scheme of \mathbf{R} and \mathbf{j} relative to the principal axis with the largest moment of inertia for a) the cranking picture, and b) the wobbling mode. The subscripts “f” and “u” refer to favoured and unfavoured couplings, with alternate signatures. In the wobbling mode, the states with spin $I, I - 1$ and $I + 1$, and $I + 2$ correspond to $n_w = 0, 1$ and 2 , respectively.

in addition to the collective angular momentum is different from the original picture presented for an even-even system [13]. Here, the total angular momentum is tilted away from the axis of the largest moment of inertia by a “wobbling angle” which increases with n_w . In the presence of an aligned particle with intrinsic angular momentum \mathbf{j} the wobbling mode is entirely related to the collective angular momentum \mathbf{R} with $\mathbf{I} = \mathbf{R} + \mathbf{j}$. The difference in the coupling scheme between the wobbling mode and the conventional cranking picture is illustrated in fig. 6.

The presence of aligned particles favors a particular (triaxial) shape and produces a unique pattern of electromagnetic transitions between the bands. The decomposition of the collective angular momentum shown in fig. 7 has been calculated with a model in which the aligned particle is coupled to a triaxial rotor [25]. The lowest solution with positive parity and favored signature ($\alpha = +1/2$), f1, has the collective angular momentum fully aligned with the x -axis (of largest moment of inertia). This solution is identified with TSD1 in ^{163}Lu . The second lowest solution obtained with $(\pi, \alpha) = (+, +1/2)$, f2, has a considerably smaller expectation value of the component R_x than f1. For the lowest solution with positive parity and unfavored signature, ($\alpha = -1/2$), u1, the expectation value of R_x is intermediate between f1 and f2, thus bearing out the expected increase in wobbling angle, here for the collective part of the angular momentum, as illustrated in fig. 6.

The most crucial information from the particle-rotor calculations of ref. [25] is contained in the size of the electromagnetic transition matrix elements. In particular, the values of $B(E2, n_w = 1 \rightarrow n_w = 0)$ are around 22–30% of the $B(E2, n_w = 1 \rightarrow n_w = 1)$ values for the collective in-band transitions in the spin-range covered by the experiment. Furthermore, with a wobbling

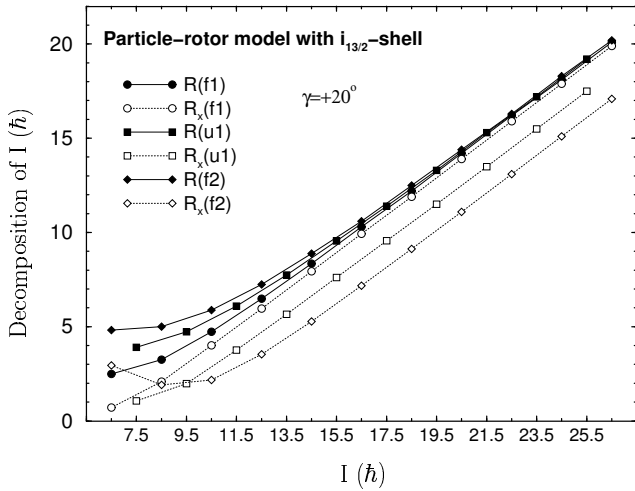


Fig. 7. Calculated expectation values of the collective angular momentum and its projection on the x -axis for the lowest favored (f1, f2) and unfavored (u1) bands in ^{163}Lu . Here f1, u1 and f2 correspond to $n_w = 0, 1$ and 2 , respectively [12, 25].

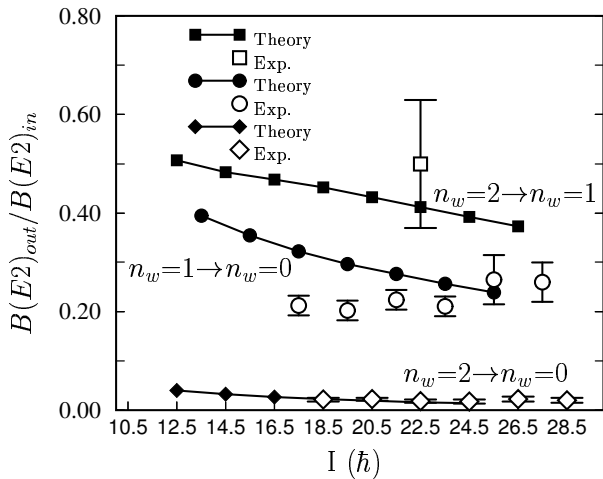


Fig. 8. Experimental and theoretical values of $B(E2)_{\text{out}}/B(E2)_{\text{in}}$. TSD1, TSD2 and TSD3 are identified with $n_w = 0, 1$ and 2 , respectively [12].

phonon description it is expected that $B(E2, n_w = 2 \rightarrow n_w = 1) \sim 2 \cdot B(E2, n_w = 1 \rightarrow n_w = 0)$. The values of $B(E2, n_w = 2 \rightarrow n_w = 0)$ are small and only nonzero due to anharmonicity in the quanta phonon description.

The data for ^{163}Lu are compared to calculations in fig. 8. The agreement illustrated in the figure, together with difficulties in alternative interpretations of the large $B(E2)$ values for the transitions TSD2 \rightarrow TSD1, and, in particular the crucial TSD3 \rightarrow TSD2 transition, provides the evidence for the wobbling excitation mode in ^{163}Lu with one- and two-phonon excitations established.

The candidate bands for the one-phonon wobbling excitation in $^{165,167}\text{Lu}$ [17, 19] show electromagnetic decay properties similar to those for TSD2 \rightarrow TSD1 in ^{163}Lu , supporting the evidence for the presence of wobbling and thereby triaxiality in these Lu nuclei.

4 Summary and outlook

A very interesting region of triaxial shapes has been revealed. Stable triaxiality is evident from the presence of 1st and 2nd phonon wobbling excitations in ^{163}Lu . This observation is further supported by the observation of wobbling phonon excitations in $^{165,167}\text{Lu}$, neighbors to ^{163}Lu , which confirms wobbling as a general phenomenon. It is still a challenge, though, to establish a wobbling excitation in an even-even nucleus without particle alignment in addition to the collective angular momentum. Yet at the spin values relevant for stable triaxial shapes some alignment which will destroy the possibility to study the “pure” textbook wobbling, is probably unavoidable. The observed wobbling frequency carries information on the distribution of the nuclear moments of inertia related to the three principal axes. They are dynamical quantities which through spectra of wobbling excitations may be studied. The present results indicate that a spin dependence is playing a role. This region of triaxiality provides the possibility of studying coexistence not only between different shapes, but also between the “normal” cranking solutions in the strongly deformed triaxial well and the wobbling quantal phonon excitation which represents a different manifestation of the rotational degree of freedom, realized in a triaxial nuclear quantal system.

In addition to the particle-rotor calculations which provide the basis for our evidence for the observation of wobbling phonon excitations, alternative theoretical formulations, for example using the cranked shell model plus random-phase approximation [28] now exist. Other attempts from nuclear-structure theory are underway [29].

The author is grateful to her many close collaborators on the research related to nuclear triaxiality and the wobbling phenomenon, in particular I. Hamamoto, D.R. Jensen, P. Bringel, G. Schönwaßer, A. Neuffer, and H. Amro, for fruitful discussions and communication of results prior to publication.

References

1. S. Åberg, Nucl. Phys. A **520**, 35c (1990) and references therein.
2. I. Ragnarsson, Phys. Rev. Lett. **62**, 2084 (1989).
3. T. Bengtsson, Nucl. Phys. A **496**, 56 (1989); **512**, 124 (1990).
4. R. Bengtsson, www.matfys.lth.se/~ragnar/ultimate.html.
5. H. Schnack-Petersen, R. Bengtsson, R.A. Bark, P. Bosetti, A. Brockstedt, H. Carlsson, L.P. Ekström, G.B. Hagemann, B. Herskind, F. Ingelbretsen, H.J. Jensen, S. Leoni, A. Nordlund, H. Ryde, P.O. Tjøm, C.X. Yang, Nucl. Phys. A **594**, 175 (1995).
6. R. Bengtsson, Hans Ryde, *Magic gaps and intruder levels in triaxially superdeformed nuclei*, to be published.
7. W. Schmitz, C.X. Yang, H. Hübel, A.P. Byrne, R. Müsseler, N. Singh, K.H. Maier, A. Kuhnert, R. Wyss, Nucl. Phys. A **539**, 112 (1992).

8. W. Schmitz, H. Hübel, C.X. Yang, G. Baldsiefen, U. Birkental, G. Fröhlingsdorf, D. Mehta, R. Müsseler, M. Neffgen, P. Willsau, J. Gascon, G.B. Hagemann, A. Maj, D. Müller, J. Nyberg, M. Piiparinen, A. Virtanen, R. Wyss, *Phys. Lett. B* **303**, 230 (1993).
9. H. Amro, P.G. Varmette, W.C. Ma, B. Herskind, G.B. Hagemann, R.V.F. Janssens, M. Bergström, A. Bracco, M. Carpenter, J. Domscheit, S. Frattini, D.J. Hartley, H. Hübel, T.L. Khoo, F. Kondev, T. Lauritsen, C.J. Lister, B. Million, S.W. Ødegård, R.B. Piercey, L.L. Riedinger, K.A. Schmidt, S. Siem, L. Wiedenhöver, J. N. Wilson, J.A. Winger, *Phys. Lett. B* **506**, 39 (2001).
10. S.W. Ødegård, G.B. Hagemann, D.R. Jensen, M. Bergström, B. Herskind, G. Sletten, S. Törmänen, J.N. Wilson, P.O. Tjøm, I. Hamamoto, K. Spohr, H. Hübel, A. Görgen, G. Schönwasser, A. Bracco, S. Leoni, A. Maj, C.M. Petrache, P. Bednarczyk, D. Curien, *Phys. Rev. Lett.* **86**, 5866 (2001).
11. D.R. Jensen, G.B. Hagemann, I. Hamamoto, S.W. Ødegård, M. Bergström, B. Herskind, G. Sletten, S. Törmänen, J.N. Wilson, P.O. Tjøm, K. Spohr, H. Hübel, A. Görgen, G. Schönwasser, A. Bracco, S. Leoni, A. Maj, C.M. Petrache, P. Bednarczyk, D. Curien, *Nucl. Phys. A* **703**, 3 (2002).
12. D.R. Jensen, G.B. Hagemann, I. Hamamoto, S.W. Ødegård, B. Herskind, G. Sletten, J.N. Wilson, K. Spohr, H. Hübel, P. Bringel, A. Neußer, G. Schönwasser, A.K. Singh, W.C. Ma, H. Amro, A. Bracco, S. Leoni, G. Benzoni, A. Maj, C.M. Petrache, G. Lo Bianco, P. Bednarczyk, D. Curien, *Phys. Rev. Lett.* **89**, 142503 (2002).
13. A. Bohr, B.R. Mottelson, *Nuclear Structure*, Vol. II (Benjamin, Reading, MA, 1975).
14. P. Bringel, H. Hübel, H. Amro, M. Axiotis, D. Bazzacco, S. Bhattacharya, R. Bhowmik, J. Domscheit, G.B. Hagemann, D.R. Jensen, Th. Kröll, S. Lunardi, D.R. Napoli, A. Neußer, S.C. Panholi, C.M. Petrache, G. Schönwasser, A.K. Singh, C. Ur, *Eur. Phys. J. A* **16**, 155 (2003).
15. J. Domscheit, B. Angenwoort, S. Törmänen, R.A. Bark, M. Bergström, A. Bracco, R. Chapman, D.M. Cullen, C. Fahlander, S. Frattini, A. Görgen, G.B. Hagemann, A. Harsmann, B. Herskind, H. Hübel, H.J. Jensen, S.L. King, S. Lenzi, D.R. Napoli, S.W. Ødegård, C. Petrache, H. Ryde, U.J. van Severen, G. Sletten, P.O. Tjøm, C. Ur, *Nucl. Phys. A* **660**, 381 (1999).
16. S. Törmänen, S.W. Ødegård, G.B. Hagemann, A. Harsmann, M. Bergström, R.A. Bark, B. Herskind, G. Sletten, P.O. Tjøm, A. Görgen, H. Hübel, B. Angenwoort, U.J. van Severen, H. Ryde, C. Fahlander, D. Napoli, S. Lenzi, C. Petrache, C. Ur, H.J. Jensen, A. Bracco, S. Frattini, R. Chapman, D.M. Cullen, S.L. King, *Phys. Lett. B* **454**, 8 (1999).
17. G. Schönwasser, H. Hübel, G.B. Hagemann, P. Bednarczyk, G. Benzoni, G. Lo Bianco, A. Bracco, P. Bringel, R. Chapman, D. Curien, J. Domscheit, B. Herskind, D.R. Jensen, S. Leoni, W.C. Ma, A. Maj, A. Neußer, S.W. Ødegård, C. Petrache, D. Roßbach, H. Ryde, K.H. Spohr, A.K. Singh, *Phys. Lett. B* **552**, 9 (2003).
18. C.X. Yang, X.G. Wu, H. Zheng, X.A. Liu, Y.S. Chen, C.W. Shen, Y.J. Ma, J.B. Lu, S. Wen, G.S. Li, S.G. Li, G.J. Yuan, P.K. Weng, Y.Z. Liu, *Eur. Phys. J. A* **1**, 237 (1998).
19. H. Amro, W.C. Ma, G.B. Hagemann, B. Herskind, J.A. Winger, Y. Li, J. Thompson, G. Sletten, J.N. Wilson, D.R. Jensen, P. Fallon, D. Ward, R.M. Diamond, A. Görgen, A. Machiavelli, H. Hübel, J. Domscheit, I. Wiedenhöver, *Phys. Lett. B* **553**, 197 (2003).
20. Y. Li, W.C. Ma, H. Amro, D.G. Roux, G.B. Hagemann *et al.*, to be published.
21. D. Ringkjøbing Jensen, J. Domscheit, G.B. Hagemann, M. Bergström, B. Herskind, B.S. Nielsen, G. Sletten, P.G. Varmette, S. Törmänen, H. Hübel, W.C. Ma, A. Bracco, F. Camera, F. Demaria, S. Frattini, B. Million, D. Napoli, A. Maj, B.M. Nyako, D.T. Joss, M. Aiche, *Eur. Phys. J. A* **8**, 165 (2000).
22. A. Neußer, S. Bhattachary, P. Bringel, D. Curien, O. Dorvaux, J. Domscheit, G.B. Hagemann, F. Hannachi, H. Hübel, D.R. Jensen, A. Lopez-Martens, E. Mergel, N. Nenoff, A.K. Singh, *Eur. Phys. J. A* **15**, 439 (2002).
23. G. Schönwasser, H. Hübel, G.B. Hagemann, J. Domscheit, A. Görgen, B. Herskind, G. Sletten, J.N. Wilson, D.R. Napoli, C. Rossi-Alvarez, D. Bazzacco, R. Bengtsson, H. Ryde, P.O. Tjøm, S.W. Ødegård, *Eur. Phys. J. A* **13**, 291 (2002).
24. G. Schönwasser, H. Hübel, G.B. Hagemann, H. Amro, R. Clark, M. Cromaz, R.M. Diamond, P. Fallon, B. Herskind, G. Lane, W.C. Ma, A. Machiavelli, S.W. Ødegård, G. Sletten, D. Ward, J.N. Wilson, *Eur. Phys. J. A* **15**, 435 (2002).
25. I. Hamamoto, *Phys. Rev. C* **65**, 044305 (2002).
26. M.K. Djongolov, D.J. Hartley, L.L. Riedinger, F.G. Kondev, R.V.F. Janssens, K. Abu Saleem, H. Ahmad, D.L. Balabanski, M.P. Carpenter, P. Chowdhury, D.M. Cullen, M. Danchev, G.D. Dracoulis, H. El-Masri, J. Goon, A. Heinz, R.A. Kaye, T.L. Khoo, T. Lauritsen, C.J. Lister, E.F. Moore, M.A. Riley, D. Seweryniak, J. Shestakova, G. Sletten, P.M. Walker, C. Wheldon, I. Wiedenhöver, O. Zeidan, J.-Y. Zhang, *Phys. Lett. B* **560**, 24 (2003).
27. D.R. Jensen, G.B. Hagemann, B. Herskind, G. Sletten, J.N. Wilson, S.W. Ødegård, I. Hamamoto, K. Spohr, H. Hübel, P. Bringel, A. Neußer, G. Schönwasser, A.K. Singh, W.C. Ma, H. Amro, A. Bracco, S. Leoni, G. Benzoni, A. Maj, C.M. Petrache, G. Lo Bianco, P. Bednarczyk, D. Curien, *Eur. Phys. J. A* **19**, 173 (2004).
28. M. Matsuzaki, Y.R. Shimizu, K. Matsuyanagi, *Phys. Rev. C* **65**, 041303 (2002); this issue, p. 189.
29. K. Sugawara Tanabe, K. Tanabe, *Triaxial Superdeformed bands in ^{163}Lu* , in abstract collection for NS2002, p. 86, not presented.